On the approximation of Feynman-Kac path integrals

Stephen D. Bond∗, Brian B. Laird†, and Benedict J. Leimkuhler‡

∗ *University of California, San Diego, Departments of Mathematics and Chemistry, La Jolla, CA
92093, USA* ,   † *University of Kansas, Department of Chemistry, Lawrence, KS 66045, USA* ,
‡ *University of Leicester, Department of Mathematics and Computer Science, Leicester, LE1 7RH, UK*
Email: bond@ucsd.edu, blaird@ku.edu, bl12@mcs.le.ac.uk

A general framework is proposed for the numerical approximation of Feynman-Kac path integrals in the context of quantum statistical mechanics. Each infinite-dimensional path integral is approximated by a Riemann integral over a finite-dimensional Sobolev space by restricting the integrand to a subspace of all admissible paths. Through this process, a wide class of methods is derived, with each method corresponding to a different choice for the approximating subspace. It is shown that the traditional "short-time" approximation and "Fourier discretization" can be recovered by using linear and spectral basis functions respectively. As an illustration of the flexibility afforded by the subspace approach, a novel method is formulated using cubic elements and is shown to have improved convergence properties when applied to model problems.

Key Words: Feynman-Kac Path Integrals, Quantum Statistical Mechanics, Functional Integration, Path Integral Methods

1. INTRODUCTION

The path integral approach provides a powerful method for studying properties of quantum many-body systems [1]. When applied to statistical mechanics [2], each element of the quantum density matrix is expressed as an integral over all curves connecting two configurations:

$$\rho\left(\mathbf{b}, \mathbf{a}\right) = \iint_{\mathbf{a}:\mathbf{b}} \mathcal{D}\left[\mathbf{x}\left(\tau\right)\right] \exp\left\{-\frac{1}{\hbar}\Phi\left[\mathbf{x}\left(\tau\right);\beta\right]\right\}. \tag{1}$$

The symbol $\mathcal{D}\left[\mathbf{x}\left(\tau\right)\right]$ indicates that the integration is performed over the set of all differentiable curves, $\mathbf{x}: [0, \beta\hbar] \to \mathbf{R}^d$, with $\mathbf{x}\left(0\right) = \mathbf{a}$ and $\mathbf{x}\left(\beta\hbar\right) = \mathbf{b}$. The integer d reflects the dimensionality, with $d = 3N$ for a system of N-particles in 3-dimensional space. The functional Φ can be derived from the classical action by introducing a relationship between temperature and imaginary time ($it = \beta\hbar$) [1]. In this paper, we will restrict our attention to the quantum many-body system, for which Φ takes the following form:

$$\Phi\left[\mathbf{x}\left(\tau\right);\beta\right] = \int_0^{\beta\hbar} \frac{1}{2}\sum_{i=1}^d m_i \, \dot{x}_i\left(\tau\right)^2 + V\left[\mathbf{x}\left(\tau\right)\right] \mathrm{d}\tau. \tag{2}$$

Calculating the path integral in (1) is a challenging task, which in general cannot be performed analytically. It is only for simple model problems, such as quadratic potentials, that an exact solution can be obtained. For more complex systems, the path integral has traditionally been estimated using either the "short-time" approximation (STA) [3] or "Fourier discretization" (FD) [4,5]. Many authors have proposed improvements to the standard STA and FD, using techniques such as improved estimators [6,7], partial averaging [8–10], higher-order exponential splittings [11], advanced reference potentials [12], semi-classical expansions [13], and extrapolation [14]. The fundamental approach is the same in all of these methods: the path integral is reduced to a high (but finite) dimensional Riemann integral, which is then approximated using either Monte Carlo or molecular-dynamics simulation techniques.

In this paper, we investigate the discretization of path integrals by projection onto a finite dimensional subspace. The idea of approximating path integrals using a finite subset of basis functions has been suggested before in the literature. Davison was one of the first to consider the use of orthogonal function expansions in the representation of Feynman path integrals [15], although he did not explore truncating the expansion. In a related article on Wiener integration of a different class of functionals, Cameron proposed using a finite set of orthogonal basis functions, and investigated the convergence of Fourier

(spectral) elements [16]. An advantage of the subspace approach is that we need not require that the basis functions are orthogonal, allowing for the direct comparison of the STA and FD methods. This is very different from operator splitting methods, which seek higher-order approximations to the Boltzmann operator [11, 17]. We should note that Coalson explored some of the connections between the STA and FD methods [18], although using a different technique.

The real power of the subspace approach is that new methods can be readily constructed using general classes of basis functions such as orthogonal polynomials or finite elements. The structural properties of the basis functions, such as smoothness and compact support, can be varied in an effort to improve overall efficiency. In Section 3, we derive path integral methods starting from three different classes of basis basis functions. It is shown that while the first two choices (linear and spectral elements) result in known methods (STA and FD), a new method can be constructed using compactly supported (Hermite) cubic splines (HCS).

The one-dimensional harmonic oscillator is one of only a few systems for which the path integral can be evaluated exactly. In Section 4, we derive expressions for the average energy of the harmonic oscillator, using two different energy estimators (E_1 and E_2) with a general subspace method. Although both estimators converge to the exact average energy, we show that E_2 (which is based on the virial equation) is far more accurate. While the error in E_1 is first-order for all three methods, the error in E_2 is second, third, and sixth-order when it is calculated using the STA, FD, and HCS methods respectively.

In Section 5, we investigate the efficiency of the path integral methods using numerical experiments. We apply each method to the problem of calculating the average energy of a particle in a one-dimensional double well. Metropolis Monte Carlo is used to sample configurations from each approximating subspace. The efficiency of each method is measured by comparing the accuracy in the E_2 estimator as a function of (a) subspace dimension and (b) total computation time. It is shown that while the FD and HCS methods provide a similar degree of accuracy as a function of subspace dimension, the HCS method requires far less computation time. This improvement in efficiency exhibited by the HCS method is due to the compact support of the Hermite cubic basis functions.

2. PATH INTEGRAL APPROXIMATION

To illustrate how one can use a subspace approximation to discretize the quantum density matrix in (1), we start by introducing a change of variables to simplify the boundary conditions and temperature dependence for each path integral: $\mathbf{x}(\tau) = \mathbf{a} + (\mathbf{b} - \mathbf{a})\tau/\beta\hbar + \mathbf{y}(\tau/\beta\hbar)$. Since the admissible paths, $\mathbf{x}$, satisfy the boundary conditions $\mathbf{x}(0) = \mathbf{a}$ and $\mathbf{x}(\beta\hbar) = \mathbf{b}$, the reduced paths given by $\mathbf{y}$, will satisfy Dirichlet boundary conditions, $\mathbf{y}(0) = \mathbf{y}(1) = \mathbf{0}$, independent of $\mathbf{a}$, $\mathbf{b}$, and β. Introducing this change of variables into (1), results in the following:

$$\rho(\mathbf{b}, \mathbf{a}) = \iint_{0:0} \mathcal{D}\left[\mathbf{y}\left(\frac{\tau}{\beta\hbar}\right)\right] \exp\left\{\frac{1}{\hbar}\Phi\left[\mathbf{a} + (\mathbf{b} - \mathbf{a})\frac{\tau}{\beta\hbar} + \mathbf{y}\left(\frac{\tau}{\beta\hbar}\right); \beta\right]\right\}. \tag{3}$$

Note that the ith component of each reduced path $\mathbf{y}$, denoted by y_i, is a real-valued function on the interval $[0, 1]$, satisfying Dirichlet boundary conditions. For the systems considered in this article, we also require that the derivative of each y_i is measurable (i.e., square-integrable). Functions of this form are members of an infinite dimensional Sobolev space [19], defined by

$$\mathcal{S}_0^1[0, 1] = \{w \in \mathcal{C}[0, 1] \,|\, w(0) = w(1) = 0 \text{ and } \|w\|_{\mathcal{S}} < \infty\}, \tag{4}$$

where

$$\|w\|_{\mathcal{S}}^2 \equiv \int_0^1 \dot{w}(\xi)^2 + w(\xi)^2 \, \mathrm{d}\xi. \tag{5}$$

We proceed in the following manner to discretize (3): Consider a sequence of subspaces of increasing dimension $\mathcal{V}_1, \cdots, \mathcal{V}_P, \cdots \subset \mathcal{S}_0^1[0, 1]$, where each $\mathcal{V}_P$ is of dimension P. For convenience, let each subspace be defined as the span of a particular set of basis functions: $\mathcal{V}_P = \text{span}\{\psi_1, \cdots, \psi_P\}$. Now, given a component function $y_i \in \mathcal{S}_0^1[0, 1]$, we can define its projection on $\mathcal{V}_P$ uniquely by

$$y_i^{(P)}(\xi) \equiv \sum_{k=1}^{P} \alpha_{k,i} \psi_k(\xi) \,, \tag{6}$$

Using the projection $y_i^{(P)}(\xi)$ as an approximation of $y_i(\xi)$ reduces the infinite-dimensional path integral in (3) to a finite-dimensional Riemann integral over the coefficients, $\alpha_{i,k}$:

$$\rho_{(p)}(\mathbf{b}, \mathbf{a}) = \int d\boldsymbol{\alpha} \, J \exp\left\{-\frac{1}{\hbar}\Phi\left[\mathbf{a} + (\mathbf{b} - \mathbf{a})\frac{\tau}{\beta\hbar} + \mathbf{y}^{(P)}\left(\frac{\tau}{\beta\hbar}\right); \beta\right]\right\}. \tag{7}$$

Here, we have used simplified notation for the multi-dimensional integral, with $d\boldsymbol{\alpha} \equiv \prod_{k,i} d\alpha_{k,i}$. The constant J reflects the particular choice of variables, and can be readily calculated (which we show later in this section). The reader should note that (7) does not depend on the basis functions chosen to represent the approximating subspace. If both $\{\psi_1, \cdots, \psi_P\}$ and $\{\tilde{\psi}_1, \cdots, \tilde{\psi}_P\}$ span $\mathcal{V}_P$, then there is an invertible linear transformation (i.e., change of variables) $\mathbf{U}$ such that $\tilde{\boldsymbol{\alpha}} = \mathbf{U}\boldsymbol{\alpha}$.

To show in detail how subspace methods can be applied in practice, we consider the case of an N-body Hamiltonian system:

$$\hat{H} = \frac{1}{2}\sum_{i=1}^{d} m_i^{-1} \hat{p}_i^2 + V[x_1, \cdots, x_d] \ . \tag{8}$$

Here, the coordinate and momentum operators are denoted by x_i and $\hat{p}_i$ respectively. For this system the functional Φ is given by (2), which when applied to the projected path, $\mathbf{x}^{(P)}(\tau) \equiv \mathbf{a} + (\mathbf{b} - \mathbf{a})\tau/\beta\hbar + \mathbf{y}^{(P)}(\tau/\beta\hbar)$, results in

$$\Phi[\mathbf{x}^{(P)}(\tau); \beta] = \int_0^{\beta\hbar} \sum_{i=1}^{d} \frac{m_i}{2}\left[\dot{x}_i^{(P)}(\tau)\right]^2 + V[\mathbf{x}^{(P)}(\tau)] \, d\tau \ . \tag{9}$$

After expanding the τ-integrals, introducing a change of variables $\xi = \tau/\beta\hbar$, and using the boundary conditions of each ψ_k, we have

$$\Phi[\mathbf{x}^{(P)}(\beta\hbar\xi); \beta] = \sum_{i=1}^{d} \frac{m_i}{2\beta\hbar}\left\{(b_i - a_i)^2 + \vec{\alpha}_i^T \mathbf{K} \vec{\alpha}_i\right\} + \beta\hbar \int_0^1 V[\mathbf{a} + (\mathbf{b} - \mathbf{a})\xi + \mathbf{y}^{(P)}(\xi)] \, d\xi \ , \tag{10}$$

where $\vec{\alpha}_i \equiv [\alpha_{1,i} \cdots \alpha_{P,i}]^T$. The "stiffness matrix", $\mathbf{K} \in \mathbf{R}^{P \times P}$, has entries given by the inner-product

$$K_{j,k} = \int_0^1 \dot{\psi}_j(\xi) \dot{\psi}_k(\xi) \, d\xi. \tag{11}$$

Substituting (10) into (7), we obtain a simplified expression for the approximate density matrix:

$$\begin{aligned}\rho_{(p)}(\mathbf{b}, \mathbf{a}) &= J \exp\left\{-\sum_{i=1}^{d} \frac{m_i}{2\beta\hbar^2}(b_i - a_i)^2\right\} \times \\ &\int d\boldsymbol{\alpha} \exp\left\{-\sum_{i=1}^{d} \frac{m_i}{2\beta\hbar^2}\vec{\alpha}_i^T \mathbf{K}\vec{\alpha}_i - \beta \int_0^1 V[\mathbf{x}^{(P)}(\xi)] \, d\xi\right\},\end{aligned} \tag{12}$$

where $\mathbf{x}^{(P)}(\xi) = \mathbf{a} + (\mathbf{b} - \mathbf{a})\xi + \mathbf{y}^{(P)}(\xi)$. For the Fourier case, one typically calculates J by requiring that the discretization be exact when applied to an ideal gas (i.e., $V \equiv 0$) [4, 5, 15]. We can apply this same technique to a general subspace method. Assuming that K is symmetric positive definite, each integral over $\vec{\alpha}_i$ can be evaluated by diagonalizing K and applying a linear change of variables; e.g.,

$$\int \exp\{-\vec{\alpha}^T \mathbf{K}\vec{\alpha}\} \, d\vec{\alpha} = \left[\det\left(\frac{1}{\pi}K\right)\right]^{-1/2}. \tag{13}$$

Applying this formula to (12) with $V \equiv 0$ allows us to solve for J in a straightforward manner:

$$J = \prod_{i=1}^{d} \sqrt{\det \mathbf{K}} \left(\frac{m_i}{2\pi\beta\hbar^2}\right)^{\frac{P+1}{2}}. \tag{14}$$

Before discussing particular choices for basis functions, we should mention that, in general, the one-dimensional ξ-integral in (12) cannot be performed analytically. This problem has been traditionally circumvented by using a discrete approximation, such as Gaussian quadrature [5, 18]. For example, one can view the primitive STA as using the trapezoidal rule. If the quadrature scheme is of sufficiently high order its use will not reduce the asymptotic rate of convergence of the overall method. An optimal scheme must be efficient, since for nonlinear N-body systems evaluating V may be computationally expensive.
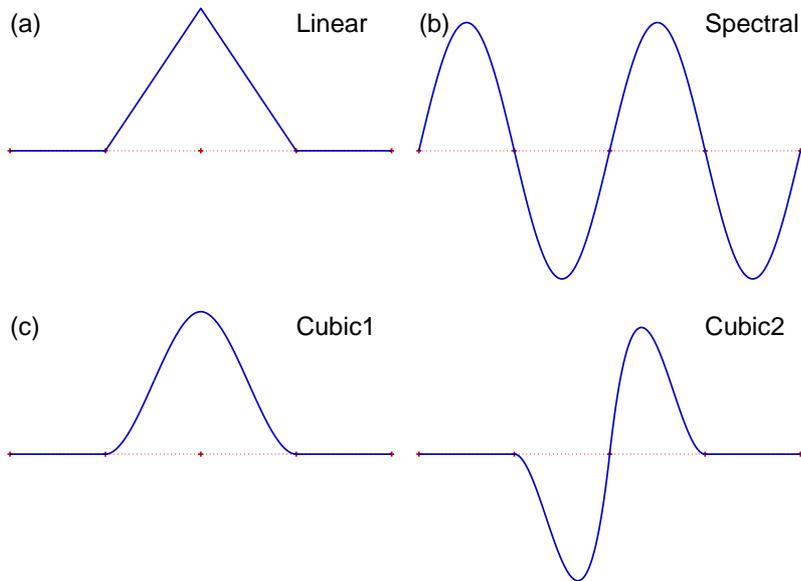
FIG. 1: Sample basis functions are shown above for the (a) linear, (b) spectral, and (c) cubic element methods.

3. SUBSPACE METHODS

As we mentioned in the previous section, the real benefit of using a general subspace approach is the flexibility afforded through the choice of basis functions. By considering a general class of pseudo-spectral or finite-element basis functions, a diverse group of discretizations can be constructed. Direct comparisons can be made between basis functions of varying smoothness and support. However, for brevity, we restrict our attention in this paper to three different types of basis functions: linear, spectral, and cubic elements. Representative basis functions from each of these discretizations are shown in Figure 1.

The traditional STA method can be constructed by considering polygonal paths, which can be represented by piecewise linear basis functions [19]. For a given number of linear segments, $P+1$, we can define an approximating subspace $\mathcal{V}_P$ as the span of basis functions $\{\psi_1, \cdots, \psi_P\}$, where each ψ_k is defined by the following formula

$$
\begin{aligned}
\psi_k(\xi) &:= \phi^{\mathrm{lin}}(\xi(P+1) - k), \\
\text{with} \quad \phi^{\mathrm{lin}}(u) &:= \begin{cases} 1 - |u| & u \in [-1, 1] \\ 0 & \text{otherwise} \end{cases}.
\end{aligned}
$$

For this discretization, one can show that the reduced path $y^{(P)}(\xi) = \sum \alpha_k \psi_k(\xi)$ satisfies Dirichlet boundary conditions, and forms a polygonal path with corners at the interior grid points $(j/(P+1), \alpha_j)$ for integers $1 \leq j \leq P$. The "stiffness" matrix, $\mathbf{K} \in \mathbf{R}^{P \times P}$, can be calculated in a routine manner, using its definition given in (11):

$$
\mathbf{K}^{\mathrm{sta}} := (P+1) \begin{bmatrix} 2 & -1 & 0 & . \\ -1 & 2 & . & 0 \\ 0 & . & 2 & -1 \\ . & 0 & -1 & 2 \end{bmatrix}. \tag{15}
$$

We should note that in the traditional formulation of the STA method, the coefficients represent points on the "true path", rather than the "reduced path". The two formulations are actually equivalent, with the coefficients related through a trivial linear change of variables.

In a similar manner, the FD method can be derived using the subspace approach by considering spectral basis functions of the form

$$
\psi_k(\xi) = \frac{1}{k} \sin(k\pi\xi). \tag{16}
$$

One attractive feature of this basis is that the stiffness matrix, $\mathbf{K} \in \mathbf{R}^{P \times P}$, is diagonal:

$$\mathbf{K}^{\mathrm{fd}} := \frac{\pi^2}{2} \begin{bmatrix} 1 & 0 & . \\ 0 & . & 0 \\ . & 0 & 1 \end{bmatrix}. \tag{17}$$

A new method can be constructed by approximating the space of paths using piecewise (Hermite) cubic splines (HCS) [19]. Each spline is defined on an interval of width $2/P$, with its shape uniquely determined by its function value and derivative at the ends of the interval. It is assumed here that P is an even integer. Each piecewise cubic path has a continuous derivative, and is described by linear combinations of the basis functions

$$\psi_k = \begin{cases} \phi_1^{\mathrm{hcs}} \left(\xi P/2 - k \right) & 1 \le k < P/2 \\ \phi_2^{\mathrm{hcs}} \left(\xi P/2 + P/2 - k \right) & P/2 \le k \le P \end{cases}, \tag{18}$$

where

$$\phi_1^{\mathrm{hcs}} (u) \quad := \quad \begin{cases} \left(1 - |u| \right)^2 \left(2 |u| + 1 \right) & u \in [-1, 1] \\ 0 & \text{otherwise} \end{cases}$$

$$\text{and} \quad \phi_2^{\mathrm{hcs}} (u) \quad := \quad \begin{cases} u \left(1 - |u| \right)^2 & u \in [-1, 1] \\ 0 & \text{otherwise} \end{cases}.$$

One can verify that the reduced path $y^{(P)}(\xi) = \sum \alpha_k \psi_k(\xi)$ satisfies Dirichlet boundary conditions, and interpolates the interior grid points $(2j/P, \alpha_j)$ for integers $1 \le j < P/2$. The derivative of the path at all the grid points is determined by the remaining $P/2 + 1$ coefficients, α_k. Due to the compact support of the basis functions, the stiffness matrix is banded, with block structure:

$$\mathbf{K}^{\mathrm{hcs}} = \frac{P}{60} \begin{bmatrix} \mathbf{K}_1 & \mathbf{K}_3 \\ \mathbf{K}_3^T & \mathbf{K}_2 \end{bmatrix}, \tag{19}$$

where the blocks are given by

$$\mathbf{K}_1 = \begin{bmatrix} 72 & -36 & 0 & . \\ -36 & 72 & . & 0 \\ 0 & . & 72 & -36 \\ . & 0 & -36 & 72 \end{bmatrix}, \quad \mathbf{K}_2 = \begin{bmatrix} 4 & -1 & 0 & . \\ -1 & 8 & . & 0 \\ 0 & . & 8 & -1 \\ . & 0 & -1 & 4 \end{bmatrix}, \tag{20}$$

$$\text{and} \quad \mathbf{K}_3 = \begin{bmatrix} -3 & 0 & 3 & 0 & . & . \\ 0 & -3 & 0 & . & . & 0 \\ 0 & . & . & 0 & 3 & 0 \\ . & . & 0 & -3 & 0 & 3 \end{bmatrix}. \tag{21}$$

Note that the blocks are not all the same size, with $\mathbf{K}_3$ of dimension $\left(\frac{P}{2} - 1 \right) \times \left(\frac{P}{2} + 1 \right)$. The determinant of $\mathbf{K}^{\mathrm{hcs}}$ may be calculated exactly, but for most purposes it is enough to know that it is a constant, which will cancel out when (12) is used to calculate averages.

4. HARMONIC OSCILLATOR

In this section we present a simple procedure for exactly evaluating the path integrals which arise when the harmonic oscillator density matrix is discretized using an arbitrary subspace method. This is one of the few cases where both the approximate and exact density matrices can be evaluated analytically. We will restrict our attention to the problem of selecting a suitable energy estimator for calculating the average energy.

The partition function is defined as the trace of the density operator:

$$Q \equiv \mathrm{Tr} \left[\hat{\rho} \right] = \int \rho \left(a, a \right) \, \mathrm{d}a. \tag{22}$$

Since the density operator is proportional to $\exp\left[-\beta\hat{H}\right]$, we can calculate the average energy by differentiating the log of the partition function with respect to β:

$$\langle E \rangle = -\frac{\partial}{\partial\beta}\ln Q = \frac{\mathrm{Tr}\left[\hat{H}\,\hat{\rho}\right]}{\mathrm{Tr}\left[\hat{\rho}\right]} = \frac{\int\left[\hat{H}\,\rho\,(x,a)\right]_{x=a}\mathrm{d}a}{\int\rho\,(a,a)\,\mathrm{d}a}. \tag{23}$$

To calculate the partition function for the approximate density matrix, $\rho_{(p)}\,(b,a)$, we start by inserting (12) into $\int\rho_{(p)}\,(a,a)\,\mathrm{d}a$:

$$Q_{(p)} = J\int\exp\left\{-\frac{m}{2\,\beta\,\hbar^2}\vec{\alpha}^T\mathbf{K}\vec{\alpha}-\beta\int_0^1 V\left[\mathbf{x}^{(P)}\,(\xi)\right]\mathrm{d}\xi\right\}\mathrm{d}\vec{\alpha}\mathrm{d}a. \tag{24}$$

Inserting the potential for the harmonic oscillator, $V\,(x) = m\,\omega^2\,x^2/2$, into the formula above results in

$$Q_{(p)} = J\int\exp\left\{-\frac{m}{2\,\beta\,\hbar^2}\vec{\alpha}^T\mathbf{K}\vec{\alpha}-\frac{\beta\,m\,\omega^2}{2}\int_0^1\left[a+\sum_{i=1}^P\alpha_i\psi_i\,(\xi)\right]^2\mathrm{d}\xi\right\}\mathrm{d}\vec{\alpha}\,\mathrm{d}a. \tag{25}$$

Expanding the quadratic term, integrating over a, and simplifying yields

$$Q_{(p)} = J\sqrt{\frac{2\,\pi}{m\,\omega^2\,\beta}}\int\exp\left\{-\frac{m}{2\,\beta\,\hbar^2}\vec{\alpha}^T\mathbf{K}\vec{\alpha}-\frac{\beta\,m\,\omega^2}{2}\vec{\alpha}^T\left(\mathbf{A}-\vec{c}\,\vec{c}^T\right)\vec{\alpha}\right\}\mathrm{d}\vec{\alpha}, \tag{26}$$

where

$$A_{i,j} = \int_0^1\psi_i\,(\xi)\,\psi_j\,(\xi)\,\mathrm{d}\xi \quad\text{and}\quad c_i = \int_0^1\psi_i\,(\xi)\,\mathrm{d}\xi. \tag{27}$$

Applying (13) to (26), we can integrate over $\vec{\alpha}$, which results in

$$Q_{(p)} = \frac{\sqrt{\det\mathbf{K}}}{\beta\,\hbar\,\omega}\left(\det\left[\mathbf{K}+(\beta\,\hbar\,\omega)^2\left(\mathbf{A}-\vec{c}\,\vec{c}^T\right)\right]\right)^{-1/2}, \tag{28}$$

where we have inserted the formula for J given in (14),

$$J = \sqrt{\det\mathbf{K}}\left(\frac{m}{2\,\pi\,\beta\,\hbar^2}\right)^{\frac{P+1}{2}}. \tag{29}$$

Distributing the determinant of $\mathbf{K}$, we can reduce (28) into the following form:

$$Q_{(p)} = \frac{1}{\beta\,\hbar\,\omega}\left(\det\left[\mathbf{I}+\mathbf{K}^{-1}\,(\beta\,\hbar\,\omega)^2\left(\mathbf{A}-\vec{c}\,\vec{c}^T\right)\right]\right)^{-1/2}. \tag{30}$$

Using the eigenvalues of $\mathbf{K}^{-1}\left(\mathbf{A}-\vec{c}\,\vec{c}^T\right)$,

$$\{\lambda_1,\cdots,\lambda_P\} = \mathrm{spec}\left[\mathbf{K}^{-1}\left(\mathbf{A}-\vec{c}\,\vec{c}^T\right)\right], \tag{31}$$

we can reduce $Q_{(p)}$ into its final form

$$Q_{(p)} = \frac{1}{\beta\,\hbar\,\omega}\prod_{i=1}^P\left[1-(\beta\,\hbar\,\omega)^2\,\lambda_i\right]^{-1/2}. \tag{32}$$

To obtain the first energy estimator, we differentiate the logarithm of the approximate partition function with respect to β:

$$\langle E_1 \rangle_{(p)} = \frac{1}{\beta}\left[1-\sum_{i=1}^P\frac{(\beta\,\hbar\,\omega)^2\,\lambda_i}{1-(\beta\,\hbar\,\omega)^2\,\lambda_i}\right]. \tag{33}$$

In Figure 2, a plot of $\langle E_1\rangle/(\hbar\omega)$ is shown as a function of $T/(\hbar\omega)$, using linear elements with $P = 8$, 16, 32, and 64. For non-zero temperatures, we find that this energy estimator converges to the true energy
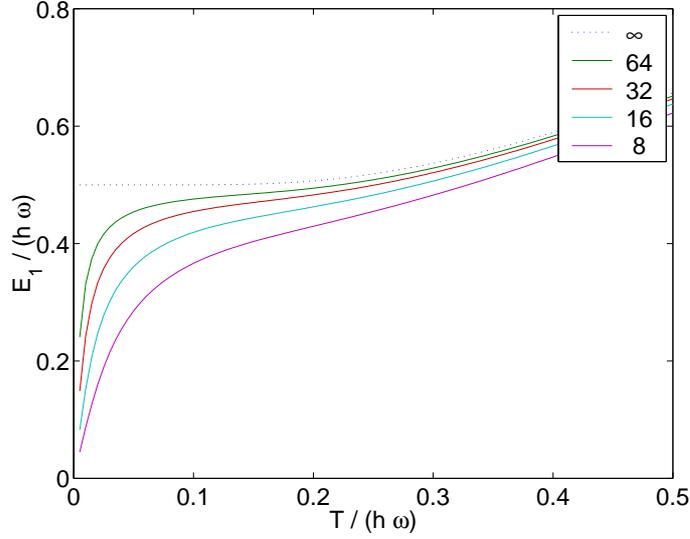
FIG. 2 Average energy as a function of temperature for the one-dimensional harmonic oscillator. The average energy is calculated using the energy estimator $\langle E_1 \rangle$ and linear elements, with $P = 8$, 16, 32, and 64. The dotted line represents the exact value, $P = \infty$.

(represented by the dotted curve) as P is increased. This estimator provides a reasonable approximation to the exact energy curve for temperatures sufficiently far from the zero-point.

A popular method for calculating the average energy can be derived using the virial theorem [6],

$$\langle E \rangle = \frac{1}{2} \langle x \, V'(x) \rangle + \langle V(x) \rangle. \tag{34}$$

For the harmonic oscillator, this means that the total average energy is simply twice the average of the potential energy. To obtain a second energy estimator, we find the average of the virial equation using the approximate density function:

$$\langle E_2 \rangle_{(p)} = \frac{1}{Q_{(p)}} \int \left[V(a) + \frac{1}{2} a \, V'(a) \right] \rho_{(p)}(a, a) \, \mathrm{d}a. \tag{35}$$

Inserting the potential for the harmonic oscillator, we find

$$\langle E_2 \rangle_{(p)} = \frac{J}{Q_{(p)}} \int m \, \omega^2 a^2 \exp \left\{ -\frac{m}{2\,\beta\,\hbar^2} \vec{\alpha}^T \mathbf{K} \vec{\alpha} - \frac{\beta\,m\,\omega^2}{2} \int_0^1 \left[a + \sum_{i=1}^{P} \alpha_i \psi_i(\xi) \right]^2 \mathrm{d}\xi \right\} \mathrm{d}\vec{\alpha} \, \mathrm{d}a. \tag{36}$$

Expanding the quadratic, integrating over a, and simplifying results in

$$
\begin{aligned}
\langle E_2 \rangle_{(p)} = \;& \frac{J}{Q_{(p)}\,\beta} \sqrt{\frac{2\,\pi}{\beta\,m\,\omega^2}} \int \left[1 + \beta\,m\,\omega^2\,\vec{\alpha}^T \vec{c}\,\vec{c}^T \vec{\alpha} \right] \\
& \times \exp \left\{ -\frac{m}{2\,\beta\,\hbar^2} \vec{\alpha}^T \left[\mathbf{K} + (\beta\,\hbar\,\omega)^2 \left(\mathbf{A} - \vec{c}\,\vec{c}^T \right) \right] \vec{\alpha} \right\} \mathrm{d}\vec{\alpha}.
\end{aligned}
\tag{37}
$$

To rewrite (37) in the form of a Gaussian integral, we insert (26) for $Q_{(p)}$ and introduce a dummy variable, γ:

$$\langle E_2 \rangle_{(p)} = \frac{1}{\beta} + \frac{2}{\beta} \frac{\partial}{\partial \gamma} \ln \left| \int \exp \left\{ -\frac{m}{2\,\beta\,\hbar^2} \vec{\alpha}^T \mathbf{K} \vec{\alpha} - \frac{m}{2\,\beta\,\hbar^2} \, (\beta\,\hbar\,\omega)^2 \, \vec{\alpha}^T \left[\mathbf{A} - \gamma\,\vec{c}\,\vec{c}^T \right] \vec{\alpha} \right\} \mathrm{d}\vec{\alpha} \right|_{\gamma=1}. \tag{38}$$

Applying (13), we can integrate over $\vec{\alpha}$ which results in

$$\langle E_2 \rangle_{(p)} = \frac{1}{\beta} - \frac{1}{\beta} \frac{\partial}{\partial \gamma} \ln \left| \det \left[\mathbf{K} + (\beta\,\hbar\,\omega)^2 \, \left(\mathbf{A} - \gamma\,\vec{c}\,\vec{c}^T \right) \right] \right|_{\gamma=1}. \tag{39}$$
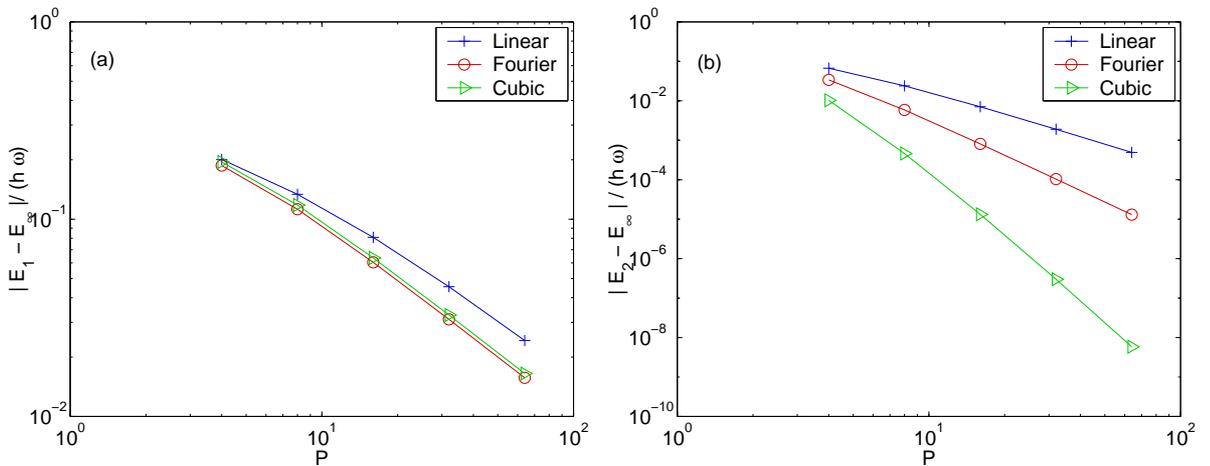
7

FIG. 3 Results for the harmonic oscillator at a temperature of $T = 0.1\hbar\omega/k_{\mathrm{B}}$. The error in the average energy is shown as a function of P, using (a) E_1 and (b) E_2 for the energy estimator. The pluses, circles, and triangles represent results using linear, Fourier, and cubic elements respectively.

Factoring out the constant $\det\left[\mathbf{K} + (\beta\hbar\omega)^2\,\mathbf{A}\right]$ from the inside of the determinant, we find

$$\langle E_2\rangle_{(p)} = \frac{1}{\beta} - \frac{1}{\beta}\frac{\partial}{\partial\gamma}\ln\left|\det\left[\mathbf{I} - \gamma\left(\mathbf{K} + (\beta\hbar\omega)^2\,\mathbf{A}\right)^{-1}\vec{c}\,\vec{c}^T\right]\right|_{\gamma=1}. \tag{40}$$

To reduce $\langle E_2\rangle_{(p)}$ into its final form, we evaluate the determinant, and differentiate with respect to γ. Note that the matrix $\left(\mathbf{K} + (\beta\hbar\omega)^2\,\mathbf{A}\right)^{-1}\vec{c}\,\vec{c}^T$ is rank-one, with a single non-zero eigenvalue of $\lambda = \vec{c}^T\left(\mathbf{K} + (\beta\hbar\omega)^2\,\mathbf{A}\right)^{-1}\vec{c}$. Applying this to (40), we are left with

$$\langle E_2\rangle_{(p)} = \frac{1}{\beta\left[1 - (\hbar\omega\beta)^2\,\vec{c}^T\left(\mathbf{K} + (\hbar\omega\beta)^2\,\mathbf{A}\right)^{-1}\vec{c}\right]}. \tag{41}$$

In Figure 3, we show the error in the average energy of the harmonic oscillator as a function of P, using linear, Fourier, and cubic elements. The average energy is calculated using (a) E_1 and (b) E_2, at a fixed temperature of $T = 0.1\hbar\omega/k_{\mathrm{B}}$. We find that the E_1 estimator is accurate to first-order in $1/P$ for all three methods. On the other hand, the E_2 estimator is far more accurate, with a convergence rate of second, third, and sixth-order for the linear, Fourier, and cubic elements respectively. Although we can't expect sixth-order for a general system, this result suggests that we may be able to do better than first-order for specific systems, depending on the estimator used to calculate thermodynamic averages.

One of the more interesting features of purely harmonic systems is that they can be used to define a reference potential for more complex systems. If the actual system is strongly harmonic, one can expect improvements in efficiency over a more traditional method which uses the "free-particle" as its reference system [4]. To illustrate how this is accomplished for a one dimensional system, with a general subspace method, we start by adding and subtracting the potential for the harmonic oscillator in (24):

$$Q_{(p)} = J\int\exp\left\{-\frac{m}{2\beta\hbar^2}\vec{\alpha}^T\mathbf{K}\vec{\alpha} - \frac{\beta m\omega^2}{2}\int_0^1\mathbf{x}^{(P)}(\xi)^2\,\mathrm{d}\xi - \beta\int_0^1\Delta V\left[\mathbf{x}^{(P)}(\xi)\right]\mathrm{d}\xi\right\}\mathrm{d}\vec{\alpha}\mathrm{d}a, \tag{42}$$

where the perturbed potential is defined as $\Delta V(x) = V(x) - m\omega^2 x^2/2$. After expanding the quadratic term, and some simplification, we are left with:

$$Q_{(p)} = J\int\exp\left\{-\frac{m}{2\beta\hbar^2}\left[\vec{\alpha}^T\mathbf{B}\vec{\alpha} + (\beta\hbar\omega a)^2\right] - \beta\int_0^1\Delta V\left[\mathbf{x}^{(P)}(\xi)\right]\mathrm{d}\xi\right\}\mathrm{d}\vec{\alpha}\mathrm{d}a. \tag{43}$$

We have combined the stiffness and mass matrices into a single positive-definite matrix, $\mathbf{B} := \mathbf{K} + (\beta\hbar\omega)^2\left[\mathbf{A} - \vec{c}\vec{c}^T\right]$. One could further reduce (43) by replacing $\mathbf{B}$ by its Cholesky factorization, which in turn induces a linear change of variables. Discussion of how, in the Fourier case, these new variables relate to "distorted waves" can be found in an article by Miller [4].
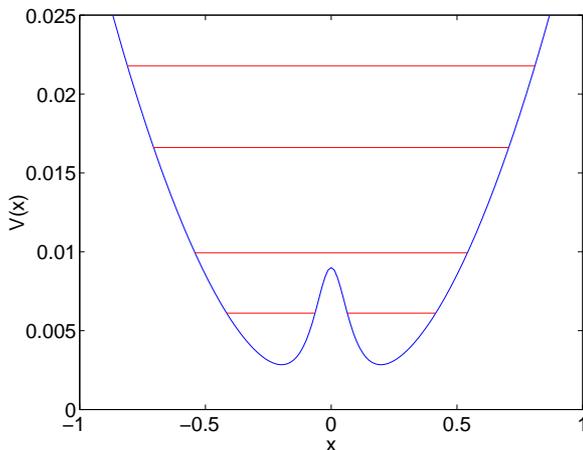
FIG. 4: The double well potential energy function in atomic units. The horizontal bars illustrate the first four energy levels, with the lowest energy state below the energy barrier.

5. DOUBLE WELL POTENTIAL: A NUMERICAL EXPERIMENT

As a numerical experiment, we apply each path integral discretization to the problem of calculating the average energy of a particle in a one-dimensional double-well. We have chosen the same double-well potential considered in [5], which is as follows:

$$V(x) = \frac{1}{2} m \omega^2 x^2 + \frac{A}{(x/a)^2 + 1}. \tag{44}$$

The parameter values are all in atomic units, with $\omega = 0.006$, $A = 0.009$, $a = 0.09$, and $m = 1836$. At low temperatures, the energy is just above 0.006, which is below the barrier height of 0.009. The potential energy, and the first four energy levels, are shown in Figure 4.

To measure the accuracy of each method, we compute the energy at a fixed temperature of $T = 0.1\hbar\omega/k$, using Metropolis Monte Carlo to generate the canonically distributed configurations. The one-dimensional line-integrals of the potential are approximated using Simpson's rule for the FD and HCS methods, and the traditional trapezoidal rule for the STA method. The number of integration nodes is set equal to the number of basis functions, P, resulting in the same number of potential evaluations for each method. For the STA method this results the potential is evaluated at the end points of each polygonal segment (consistent with its traditional implementation).

Since the aim of our numerical experiments is to measure the accuracy of the discretization, no attempt is made to optimize the efficiency of the Monte Carlo algorithm. While the application of more advanced sampling techniques such as staging [20], and harmonic reference potentials [4] would certainly improve the sampling efficiency for this problem, this would not improve the accuracy of the underlying discretization.

It has been previously observed that averaged quantities (such as energy) converge at different rates, depending on the system, reference potential, and the form of the estimator [5, 6, 21]. We use a virial estimator of the energy [6],

$$E_2 = \langle V(x) + \frac{1}{2} x V'(x) \rangle, \tag{45}$$

which was shown to exhibit improved convergence properties in the previous section. The accuracy of each average is determined by comparing with the "exact" solution, computed by summing over the 15 lowest energy levels as calculated with Numerov's method [22].

In Fig. 5, the error in the computed energy is shown as a function of (a) the number of basis functions and (b) normalized CPU time. When the number of basis functions (or potential evaluations) is used as a measure of the work, we find that the FD and HCS methods are comparable, and both are more efficient than the STA method. However, when compared on the basis of CPU time, the HCS method is dramatically more efficient than both other methods. The inefficiency of the FD method for low-dimensional problems can be explained by considering the work required to compute P points on the path. This work scales like $O(P^2)$ for the FD method, since the spectral basis functions are not compactly
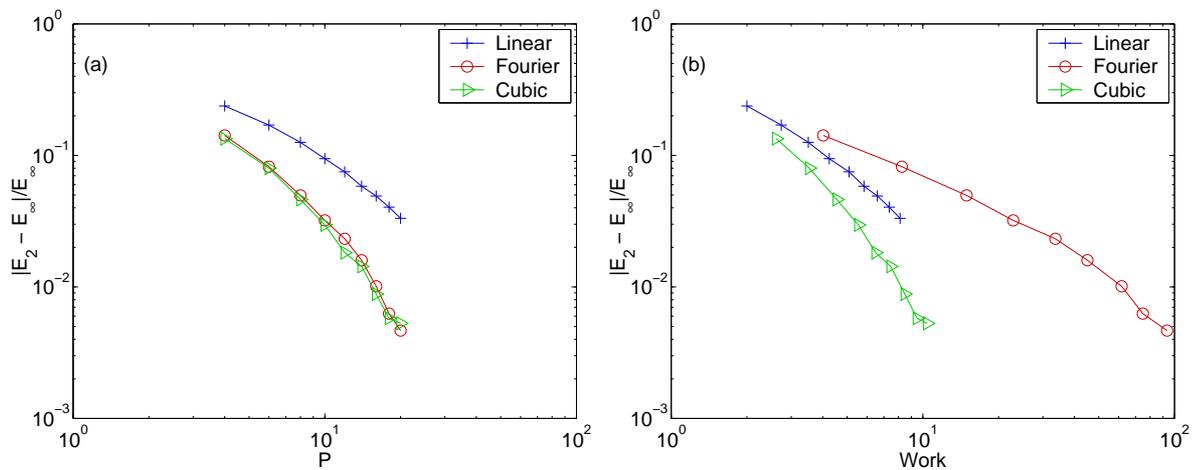
FIG. 5: Results for the double well at a temperature of $T = 0.1\hbar\omega/k_{\mathrm{B}}$. The difference between $\langle E_2 \rangle$ and the exact average energy is shown as a function of (a) subspace dimension, P and (b) CPU time (work). The pluses, circles, and triangles represent results using linear, Fourier, and cubic elements respectively.

supported. On the other hand, for the STA and HCS methods this cost scales linearly with P. Although for very high-dimensional problems, the cost of evaluating the potential should dominate, and we expect that the differences in computational cost would not be as pronounced.

6. CONCLUSION

We show that the problem of approximating Feynman-Kac path integrals can be addressed using the finite-dimensional subspace approach. This general framework allows for the ready construction of broad classes of new methods through the choice of a suitable set of basis functions. In addition, traditional approaches, such as the short-time approximation and Fourier discretization methods, can be formulated and compared using this formalism. As an illustration, we demonstrate that, by considering Hermite cubic splines (HCS), a new method can be constructed that exhibits dramatically improved efficiency over standard methods when applied to two one-dimensional model problems: the harmonic oscillator and an anharmonic double-well. Of course, whether this improvement over standard methods can be sustained in applications to the more complex multi-dimensional problems of interest in chemistry and physics is as yet an open question; however, the enhancement seen in the one-dimensional problems is significant enough to warrant further study. In addition, it must be pointed out that the HCS discretization is only one of infinitely many possible methods that can be constructed within the generalized subspace formalism approach presented here.

7. ACKNOWLEDGEMENTS

REFERENCES

[1] R. P. Feynman and A. R. Hibbs, *Quantum Mechanics and Path Integrals* (McGraw-Hill, New York, 1965).

[2] R. P. Feynman, *Statistical Mechanics* (Benjamin, Reading, Mass., 1972).

[3] K. S. Schweizer, R. M. Stratt, D. Chandler, and P. G. Wolynes, J. Chem. Phys. **75**, 1347 (1981).

[4] W. H. Miller, J. Chem. Phys. **63**, 1166 (1975).

[5] D. L. Freeman and J. D. Doll, J. Chem. Phys. **80**, 5709 (1984).

[6] M. F. Herman, E. J. Bruskin, and B. J. Berne, J. Chem. Phys. **76**, 5150 (1982).

[7] C. Chakravarty, M. C. Gordillo, and D. M. Ceperley, J. Chem. Phys. **109**, 2123 (1998).

[8] J. D. Doll, R. D. Coalson, and D. L. Freeman, Phys. Rev. Lett. **55**, 1 (1985).

[9] R. D. Coalson, D. L. Freeman, and J. D. Doll, J. Chem. Phys. **85**, 4567 (1986).

[10] R. D. Coalson, D. L. Freeman, and J. D. Doll, J. Chem. Phys. **91**, 4242 (1989).

[11] H. De Raedt and B. De Raedt, Phys. Rev. A **28**, 3575 (1983).

[12] M. Takahashi and M. Imada, J. Phys. Soc. Jpn. **53**, 3765 (1984).

[13] N. Makri and W. H. Miller, J. Chem. Phys. **90**, 904 (1989).

[14] S. L. Mielke, J. Srinivasan, and D. G. Truhlar, J. Chem. Phys. **112**, 8758 (2000).

[15] B. Davison, Proc. Roy. Soc. London Ser. A **225**, 252 (1954).

[16] R. H. Cameron, Duke Math. J. **18**, 111 (1951).

[17] M. Suzuki, Commun. math. Phys. **51**, 183 (1976).

[18] R. D. Coalson, J. Chem. Phys. **85**, 926 (1986).

[19] G. Strang and G. J. Fix, *An Analysis of the Finite Element Method* (Prentice-Hall, Englewood Cliffs, N.J., 1973).

[20] E. L. Pollock and D. M. Ceperley, Phys. Rev. B **30**, 2555 (1984).

[21] M. Eleftheriou, J. D. Doll, E. Curotto, and D. L. Freeman, J. Chem. Phys. **110**, 6657 (1999).

[22] I. N. Levine, *Quantum Chemistry*, fifth ed. (Prentice Hall, Upper Saddle River, N.J., 2000).